AIP Journal of Applied Physics

Multiple Fano interferences in a plasmonic metamolecule consisting of asymmetric metallic nanodimers

Khai Q. Le, Andrea Alù, and Jing Bai

Citation: Journal of Applied Physics **117**, 023118 (2015); doi: 10.1063/1.4905619
View online: http://dx.doi.org/10.1063/1.4905619
View Table of Contents: http://scitation.aip.org/content/aip/journal/jap/117/2?ver=pdfcov
Published by the AIP Publishing

JOURNAL OF APPLIED PHYSICS **117**, 023118 (2015)

Multiple Fano interferences in a plasmonic metamolecule consisting of asymmetric metallic nanodimers

Khai Q. Le,[1,2,a)] Andrea Alù,[3] and Jing Bai[2]
[1]*Faculty of Science and Technology, Hoa Sen University, Ho Chi Minh, Vietnam*
[2]*Department of Electrical Engineering, University of Minnesota, Duluth, Minnesota 55812, USA*
[3]*Department of Electrical and Computer Engineering, University of Texas at Austin, Austin, Texas 77812, USA*

(Received 31 October 2014; accepted 26 December 2014; published online 14 January 2015)

We theoretically explore signatures of plasmonic Fano interferences in a subwavelength plasmonic metamolecule consisting of closely packed asymmetric gold nanodimers, which lead to the possibility of generating multiple Fano resonances in the scattering spectrum. This spectral feature is attributed to the interference between bright and dark plasmonic modes sustained by the constituent nanodimers. The excited Fano dips are highly sensitive in both wavelength and amplitude to geometry and background dielectric medium. The tunability of induced Fano resonances associated with enhanced electric fields from the visible to infrared region provides promising applications, particularly in refractive index sensing, light-trapping, and photon up-converting. © *2015 AIP Publishing LLC*.
[http://dx.doi.org/10.1063/1.4905619]

I. INTRODUCTION

Plasmonic Fano resonances have recently received significant research attention, because of their potential applications in chemical/biological sensing, lasing, switching, optical filters, nonlinear and slow-light optical devices that benefit from its ultra-sharp spectral features and extreme field localization.[1–11] These sharp resonances have been observed in the optical response of various complex structures including nanoparticle clusters,[2,3,12,13] dolmen-type arranged slab structures,[14,15] symmetry-broken core-shell,[16] composite cut-wire[17] and heterogeneous dimer[18–20] structures, non-concentric ring-disk cavities,[21–23] layered nanoparticles,[24–26] and others.[4,7,27] The generation of Fano resonances depends on structural geometries, which is normally caused by either the coupling between a narrow discrete resonance and a broad resonance in the optical response of metallic arrays,[4] or the interference of bright and dark plasmon modes of individual components of hybrid structures.[3] In general, it has been based on purely electric effects in the absence of natural magnetism. Recently, a novel mechanism to excite Fano resonance in the scattering spectrum of a subwavelength plasmonic metamolecule was introduced, arising from the coupling of a strong narrow magnetic resonance and a broad electric resonance.[28] The metamolecule consists of four closely packed asymmetric-arranged gold nanoparticles. The asymmetric arrangement of nanoparticles with small inter-particle gaps was demonstrated to support a strong magnetic resonance and a broad electric resonance that can couple together due to the magneto-electric coupling associated with the asymmetry. At a certain angle of light incidence, significant interaction between these spectral resonances results in a pronounced dip in the total scattering spectrum, which has allowed to demonstrate magnetic-based Fano scattering features at optical frequencies.

In this work, we further explore the consequences of plasmon interference in a plasmonic metamolecule, which may lead to multiple Fano scattering features. In contrast to magnetic-based optical Fano-resonant metamolecule consisting of asymmetric-arranged nanoparticles with small inter-particle gaps, the proposed metamolecule is made of the combination of nanoparticle dimers having different dimer's size and inter-particle gaps. Even at normal incidence, various Fano-like dips are observed in the overall scattering spectrum. This spectral feature arises from destructive interference between bright and dark plasmon modes of the dimer components of the metamolecule. These Fano resonances appear to be highly sensitive in both wavelength and magnitude to geometry and local dielectric environment. Related works have reported the formation of multiple Fano resonances in different metallic nanostructures such as asymmetric split ring resonators,[29] plasmonic oligomer clusters,[17,30,31] and monolayer hexagonal metallic shells.[32] The generation of these Fano resonances is mainly determined by symmetry breaking and bianisotropic coupling. In contrast, by simply positioning individual constituent dimer within the proposed cluster geometry, we can manipulate and control the Fano generation at the wavelength of interest, owing to the fact that the dipolar plasmon resonant mode can be easily tuned upon the size and inter-particle gap.

II. PLASMONIC METAMOLECULE

A number of computational techniques have been successfully employed to investigate the optical properties of

a)Author to whom correspondence should be addressed. Electronic mail: khai.lequang@hoasen.edu.vn

plasmonic nanostructures. These techniques include the finite difference time domain method,[33] the finite element method,[34] the boundary element method (BEM),[35,36] the method-of-moment surface integral equation,[37] etc. In this work, all simulations were carried out using the BEM method as implemented in the MATLAB-based toolbox MNPBEM[38] and adapted to solve the full-wave Maxwell's equations. The constituent nanoparticles of the proposed cluster are assumed to be gold (Au) spheres. The number of vertices used to describe the sphere is 400 for all BEM simulations. The Au permittivity with realistic material losses was interpolated from experimental data.[39] All scattering spectra were calculated for normal incidence. Quantum effects[40–43] related to non-local screening and tunneling of electrons between two neighboring nanoparticles with sub-nanometer gaps are neglected in this work.

A. Optical properties of individual constituent dimer of a metamolecule

Several important aspects of optical nanodimers have been investigated in the literature. Physical and unphysical modes of nanoparticle dimers were reported in Ref. 44. Electromagnetic interactions between two coupled nanoparticles were investigated in Refs. 45 and 46. Alù *et al.*[47] studied the input impedance, radiation resistivity, and impedance matching of plasmonic dimers. Theoretical and experimental investigations have shown the polarization dependence of gold nanoring/nanotoroid dimers.[48,49] Distance dependent quenching effects in nanoparticle dimers have been explored in Ref. 50. In this work, we are particularly interested in the tunability of the dominant dipolar plasmon resonances (DDPR) of nanoparticle dimers. Fig. 1 shows the polarization dependence of Au dimers' scattering cross-section (SCS). The parameters needed for SCS calculations are depicted in the figure. For s-polarization, for which the incident electric field is parallel to the dimer axis, the inter-particle gap g has significant effects on the dimer's DDPR. As the nanoparticles approach each other, the resonance peak tends to redshift from the visible to infrared (IR) range accompanying the gradual increase of SCS's magnitude, as shown in Fig. 1(a). When the nanoparticles are far away from each other, the resonance is close to the localized surface plasmon resonance (LSPR) of a single particle, which is the case of an isolated nanoparticle. This is consistent with previous theoretical predictions by means of various approximate models.[51–54] This is caused by the strong coupling of LSPR supported by two neighboring nanoparticles when they are in close proximity. The hot spot inside the gap between the nanoparticles as illustrated in Fig. 2(a) is an evidence for this strong interaction. With a small inter-particle gap, the field intensity is strongly enhanced. In contrast, for p-polarization where the incident electric field is perpendicular to the dimer axis, the SCS's magnitude decreases as the inter-particle gap increases, whereas the dimer's DDPR is unchanged and remains at the LSPR of the single nanoparticle, as shown in Fig. 1(b). In this case, no interaction between the nanoparticles' LSPR is observed even if the particles nearly touch, which corresponds to the dark spot in the

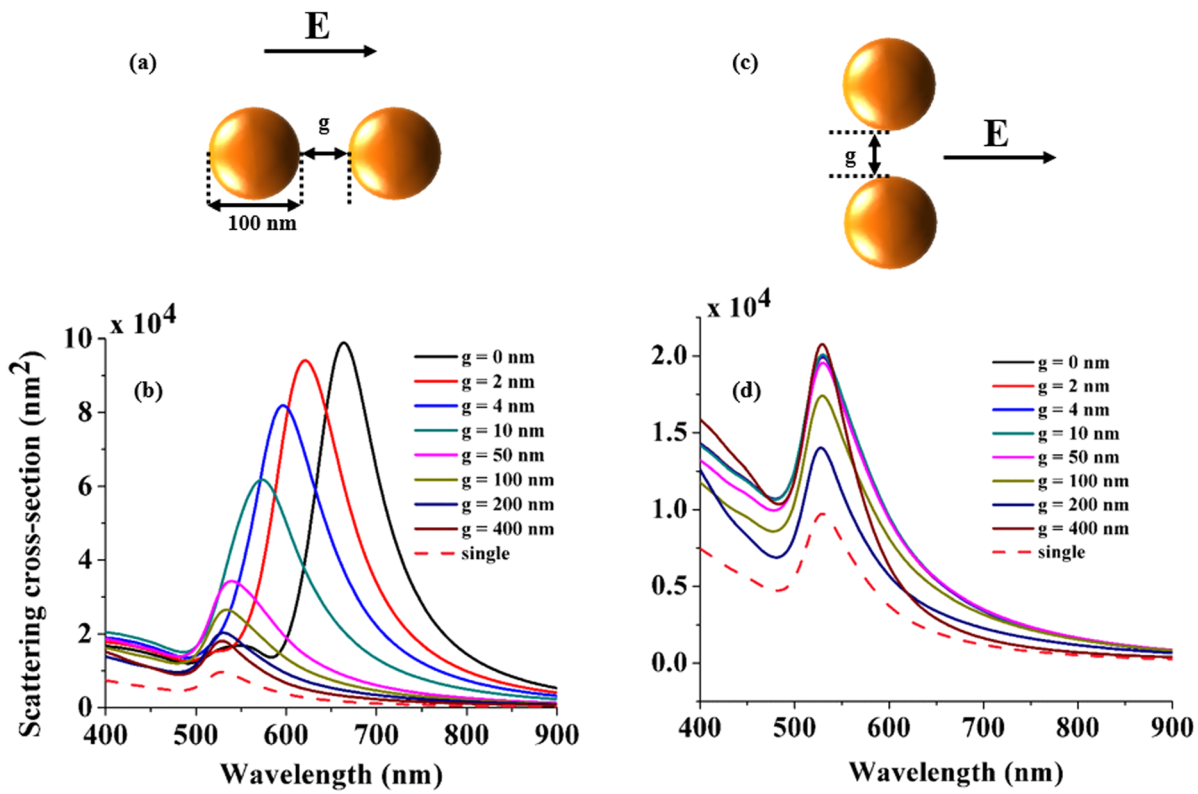

FIG. 1. Scattering cross-section of Au dimers for various inter-particle gaps g under s- and p-polarization, respectively.

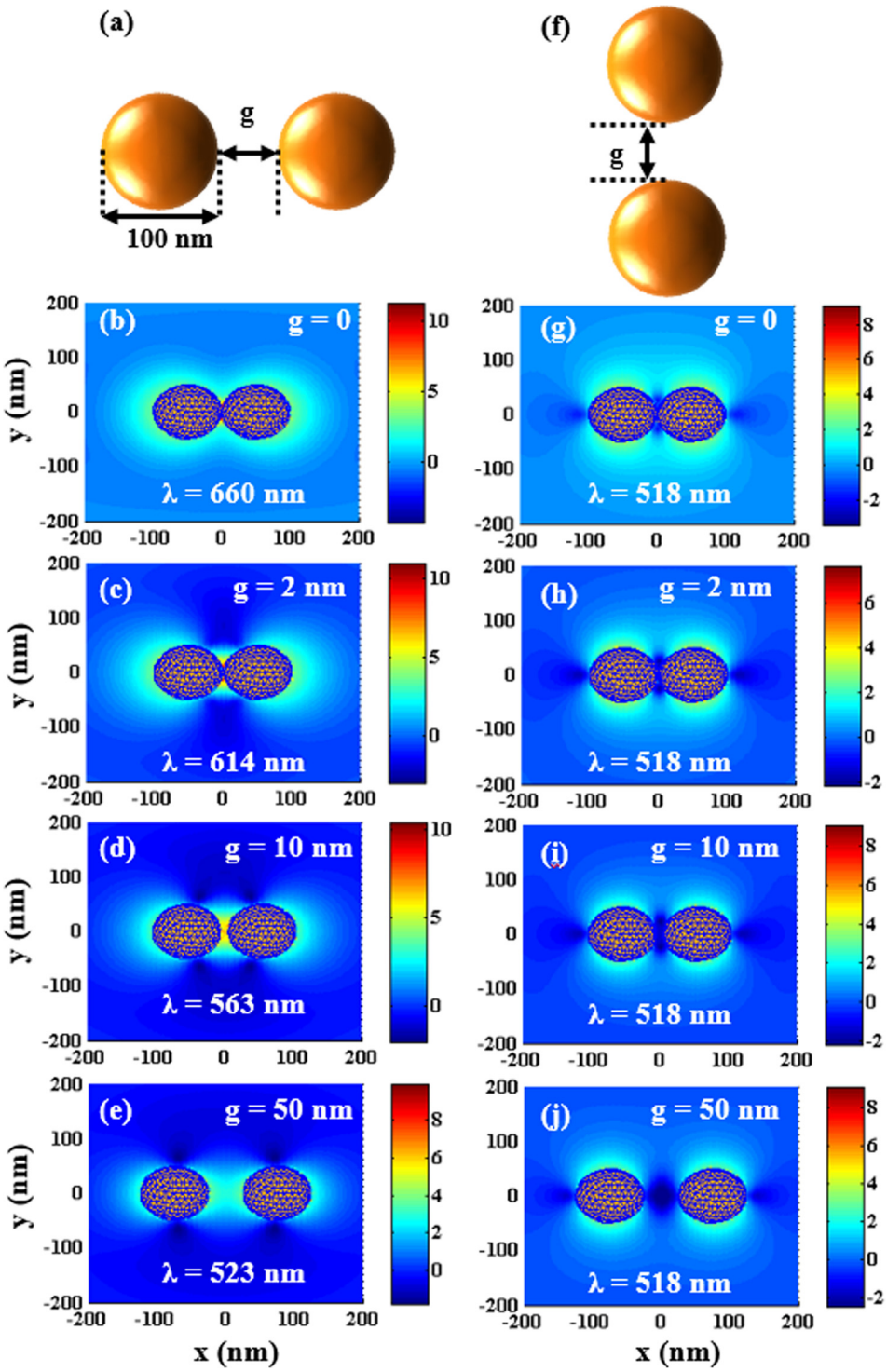

FIG. 2. Logarithm scale of electric field intensity (log ($|E|^2/|E_0|^2$)) around Au dimers for various inter-particle gaps g under s- and p-polarization, respectively.

inter-particle gap in Fig. 2(b). Since the dimer's DDPR is tunable upon the inter-particle gap under s-polarized incident light, it may be possible to generate and control Fano resonances when various dimers are coupled into a single metamolecule. We note that, if the inter-particle gap is down to sub-nanometer $g < 1$ nm, the classical model assumed in this work breaks down, and the resonance peak tends to blue-shift, potentially broadening the bandwidth and weakening the Fano signature predicted here.[43] At least qualitatively, however, we predict that the interference effects described here should hold also after considering these quantum effects.

B. A metamolecule consisting of asymmetric dimers

The symmetry breaking of the nanoparticle oligomer cluster has so far been one of the most effective techniques to excite Fano resonances. However, manipulating such resonance at wavelengths of interest is a challenge; moreover, searching for a comprehensive rule for the resonance

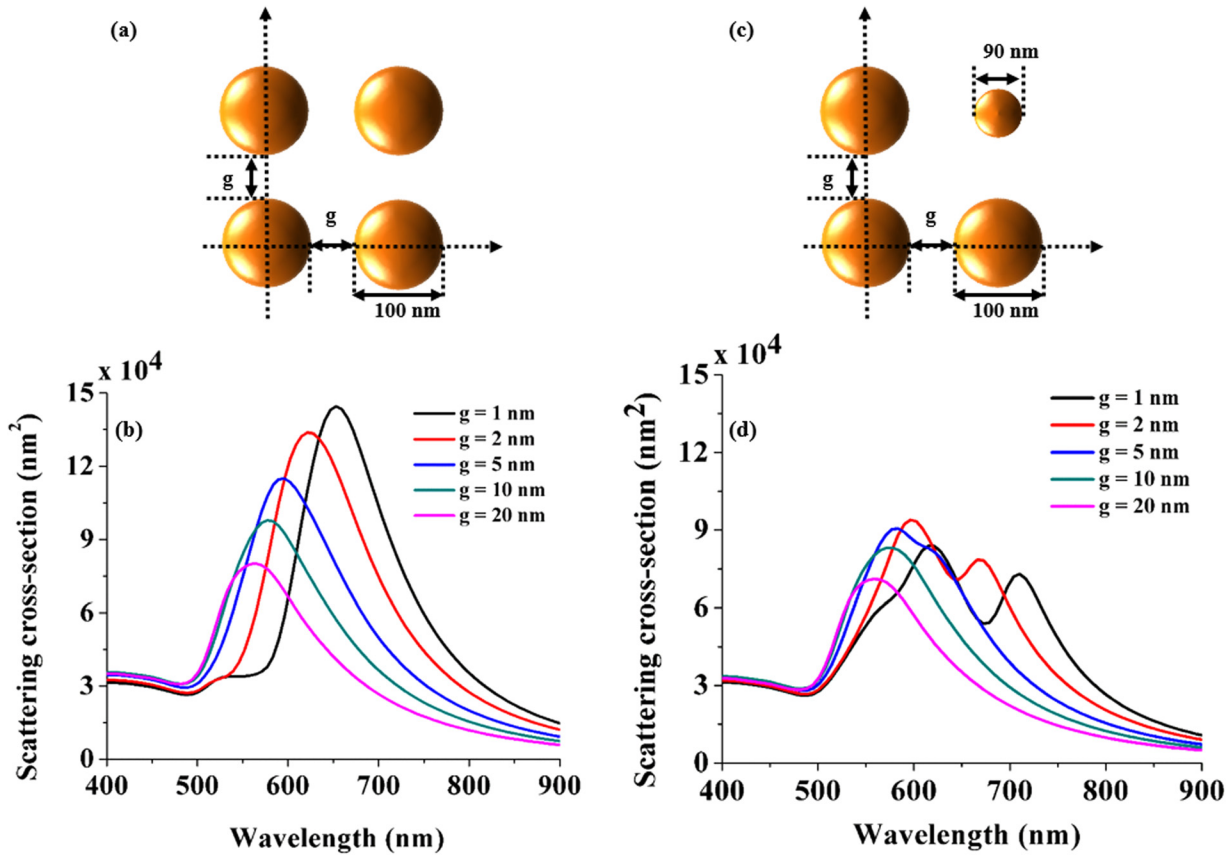

FIG. 3. Scattering cross-section of symmetric and asymmetric Au metamolecules for various inter-particle gaps g under s-polarization. Fano resonances excited by asymmetric metamolecules with small inter-particle gaps.

generation substantially adds to the design constraints. In contrast, there is a direct way to manipulate the Fano resonance generation through the proposed metamolecule consisting of coupled dimers. Since the dominant plasmon resonant (bright) and off-resonant (dark) modes of the dimer are determined by the nanoparticle size and inter-particle gap, we can control the interaction between these modes in different dimers, especially if we properly position them in close proximity, as destructive interference of their plasmonic modes can result in a Fano dip. This mechanism is verified, analyzed, and discussed in the following.

Figure 3 illustrates the SCS spectra of a metamolecule consisting of two dimers with respect to the inter-particle gaps illustrated in the panel. A metamolecule consisting of two symmetrically arranged dimers is shown in Fig. 3(a). The DDPR of the entire molecule is located exactly at the individual DDPR of the constituent dimers. Except for the increased SCS's magnitude of the metamolecule, its optical properties have the same dispersion as the individual constituent dimers. As the inter-particle gap g increases, the DDPR has a redshift toward the LSPR of a single particle and the SCS's magnitude decreases, which can be seen from Fig. 3(b). In this case, the entire molecule acts as a single isolated dimer. It is obvious that the symmetric arrangement of dimers does not result in any surprising phenomenon since the overlap of dimers' DDPR bright modes simply causes the amplification of the scattering magnitude. Nevertheless, what happens if we combine various dimers with different size and gap, introducing some inherent asymmetry into the problem? Figure 3(c) shows the metamolecule consisting of two dimers with different particle sizes. For inter-particle gaps $g > 10\,\text{nm}$, the metamolecule has the same optical properties as an isolated nanoparticle and the DDPR locates at the single nanoparticle's LSPR. In such case as well as that of the metamolecule consisting of symmetric dimers, there is a weak interaction between two constituent dimers. The dark spots in the gap between vertical particles in Figs. 4(a)–4(d) and 4(h) prove these weak interactions. In contrast, for inter-particle gaps $1\,\text{nm} \le g < 5\,\text{nm}$ signatures for strong coupling between nanodimers are observed. Within these values for the gap size, the resonant coupling can be still described using classical electromagnetic models, as done in this work, neglecting the quantum tunneling effects.[40,41] However, they may become more relevant as the inter-particle gap is reduced below 1 nm. In this case, a quantum-corrected model, which describes the junction between two neighboring nanoparticles by a nonlocal dielectric response, can be employed to describe these effects.[40] Although the optical properties of coupled nanoparticles may be varied in this regime, the basic physics behind strong coupling between these resonant modes should be preserved. It results in a Fano-like dip in the SCS spectra that can be clearly seen in Fig. 3(d).

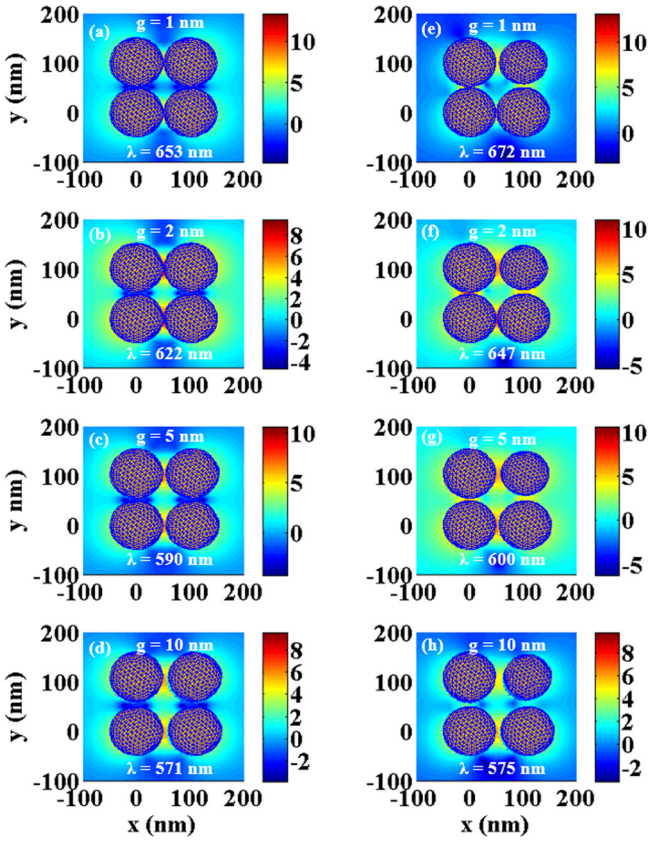

FIG. 4. Logarithm scale of relative electric field intensity (log ($|E|^2/|E_0|^2$) around (left) symmetric and (right) asymmetric Au metamolecules for various inter-particle gaps *g* under s-polarization. Strong coupling between individual dimer components with small inter-particle gaps is observed in asymmetric metamolecules, which results in Fano resonances.

The hot spots in the gap between vertical spheres are shown in Figs. 4(e)–4(g) as an evidence for this interaction. The physics behind the Fano generation is analyzed in Fig. 5. Fig. 5(a) depicts the metamolecule consisting of two asymmetric dimers with size and gap shown in the panel. While the DDPR of the top dimer shifts to the single sphere's LSPR, that of the bottom dimer shifts to the IR. As the highest bright mode of the bottom dimer couples into the low dark mode of the top dimer, the destructive interference between these modes results in a Fano dip in the SCS spectrum as seen in Figs. 5(b)–5(d). The sharpness (or Q-factor) of the Fano resonance depends on the contrast between the bright and dark modes of two dimers. For $g < 5$ nm, the higher Q-factor of the Fano dip is associated with the higher contrast between the bright and dark modes; on the other hand, for $g \geq 10$ nm no Fano dip is observed in Fig. 5(e) since the bright modes of two dimers are almost overlapped in this case. This is consistent with the analytical predictions in Ref. 55.

To further justify the interference signature, another arrangement of two different dimers is investigated, with results presented in Fig. 6. The proposed metamolecule is depicted in Fig. 6(a). Two dimers have the same size but different inter-particle gap *g*. While the inter-particle gap of the top dimer is fixed at 1 nm, that of the bottom dimer is gradually changed to shift its DDPR. Interestingly, two Fano dips occur in the SCS spectra in the 400–900 nm wavelength range as seen in Fig. 6(c). These properties reflect the fact that the Fano dips are tunable upon the gap *g*. The first Fano dip is generated by the destructive interference between the brightest mode of the bottom dimer and the dark mode of the top dimer. The second Fano dip is in contrast excited by the destructive interference between the dark mode of the bottom dimer and the brightest mode of the top dimer. For example, with the metamolecule consisting of the top dimer ($d = 100$ nm, $g = 1$ nm) and the bottom dimer ($d = 100$ nm, $g = 20$ nm) the first Fano dip at 584 nm and the second Fano dip at 660 nm are generated. It can be found that the first and second dips locate exactly at the bottom and top dimers' DDPR. Fig. 7 shows the electric intensity of the metamolecule at the two Fano dips. We can see hot spots inside the gap between vertical dimers, demonstrating the existence of strong interaction between the two constituent dimers.

Similar scenarios for Fano generation can arise in another metamolecule geometry consisting of two dimers having different nanoparticle size as considered in Fig. 8. The sketch of the metamolecule is shown in Fig. 8(a). The top dimer has particle size $d = 130$ nm and inter-particle gap $g = 1$ nm, able to blueshift the DDPR far away from the LSPR of the constituent particle. The particle size of the bottom dimer is fixed at 100 nm. Variation of the inter-particle gaps of the bottom dimer gradually redshifts the DDPRs toward the LSPR of the constituent particle. The DDPR tunability in the SCS spectra is shown in Fig. 8(b). As expected, the combination of the two dimers results in Fano dips in the SCS spectra as seen in Fig. 8(c). Considering the bottom dimer with inter-particle $g = 1$ nm, the magnitude of the SCS at the highest DDPR mode is about equal to the magnitude of the dark mode of the top dimer at the same wavelength. Therefore, the overlap of these modes does not give rise to Fano dips due to a low Q-factor. The same scenario arises when the interaction of the bright DDPR of the top dimer and the dark mode of the bottom dimer at 786 nm results in a low Q-factor Fano dip. In contrast, a pronounced Fano dip is generated when the high contrast of the bright DDPR of the top dimer and the dark mode of the bottom dimer interfere. Indeed, as the inter-particle gap *g* of the bottom dimer increases, the DDPRs are redshifted far away from the highest DDPR of the top dimer. The longer shift and higher contrast of the bright mode of the top dimer and the dark mode of the bottom dimer result in a deeper Fano dip. The hot spots of the field intensity in the gap between vertical spheres at the chosen Fano dip in the inset demonstrate strong coupling of these modes.

Up to now, we have been able to demonstrate that the interference between the bright DDPR mode and the dark mode of the two constituent dimers of the metamolecule results in a Fano resonance. The contrast of these modes in term of magnitude and wavelength shift in the SCS spectra determines the sharpness (or Q-factor) of the Fano dip. The combination of the two dimers may result in dual Fano resonances. It implies

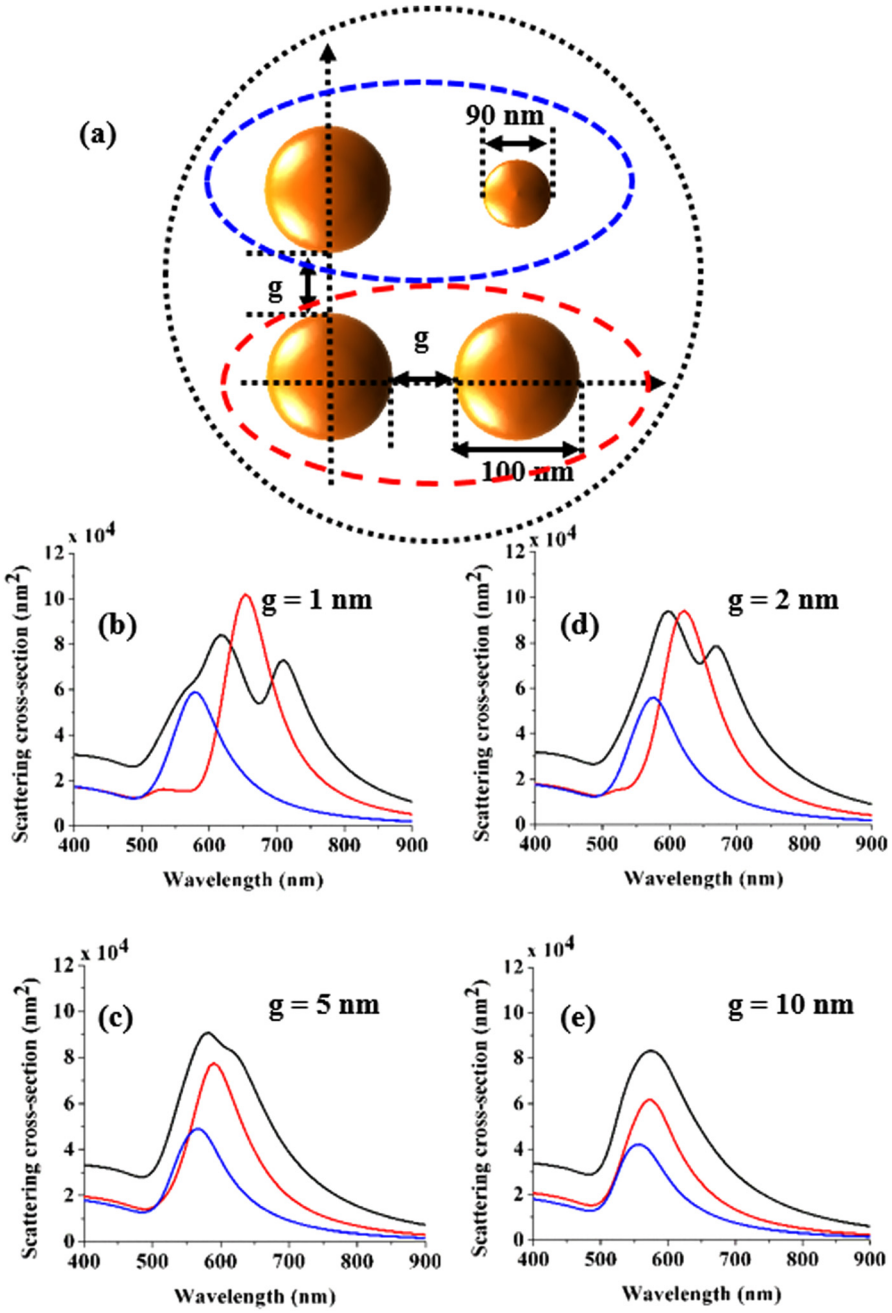

FIG. 5. Scattering cross-section of symmetric (red) and asymmetric (blue) dimer, and asymmetric metamolecules (black) for various inter-particle gaps g under s-polarization. Fano dips are excited due to the interference of bright and dark modes of individual dimer components.

that a metamolecule consisting of three dimers may possibly generate multiple Fano resonances, as presented in Fig. 9. The metamolecule consists of three dimers with different sizes as shown in Fig. 9(a). Three Fano-like dips in the SCS spectrum associated with the interference of the bright DDPR and dark modes of the constituent dimers are observed as shown in Fig. 9(b). This again verifies our vision related to Fano generation in metamolecules by properly manipulating the composition and geometry of their constituent dimers.

III. POTENTIAL APPLICATIONS OF FANO-RESONANT METAMOLECULES

Plasmonic interferences such as surface plasmon interference,[56] plasmon-plasmon interaction induced Fano resonance are strongly influenced by the electrostatic screening introduced from the surrounding environment.[21] The proposed structures may find promising applications especially in refractive index sensing,[57] light-trapping,[58] photon up-converting,[59] and others.[60] This is attributed to (i) the generation of the Fano resonance with narrow shape, (ii) the ability to tune the scattering resonances from the visible into IR region, (iii) the large enhancement of electric field in the gap between coupled particles. It can be seen from Fig. 10 that, with the chosen metamolecule geometry, the excited Fano resonance is highly sensitive to the refractive index of the local dielectric environment. The resulting sensitivity (S) at the Fano dip is about 640 nm/RIU. Apart from sensitivity, another factor determining the sensing performance is the selectivity, which refers to the figure-of-merit (FOM) defined as the ratio between sensitivity and

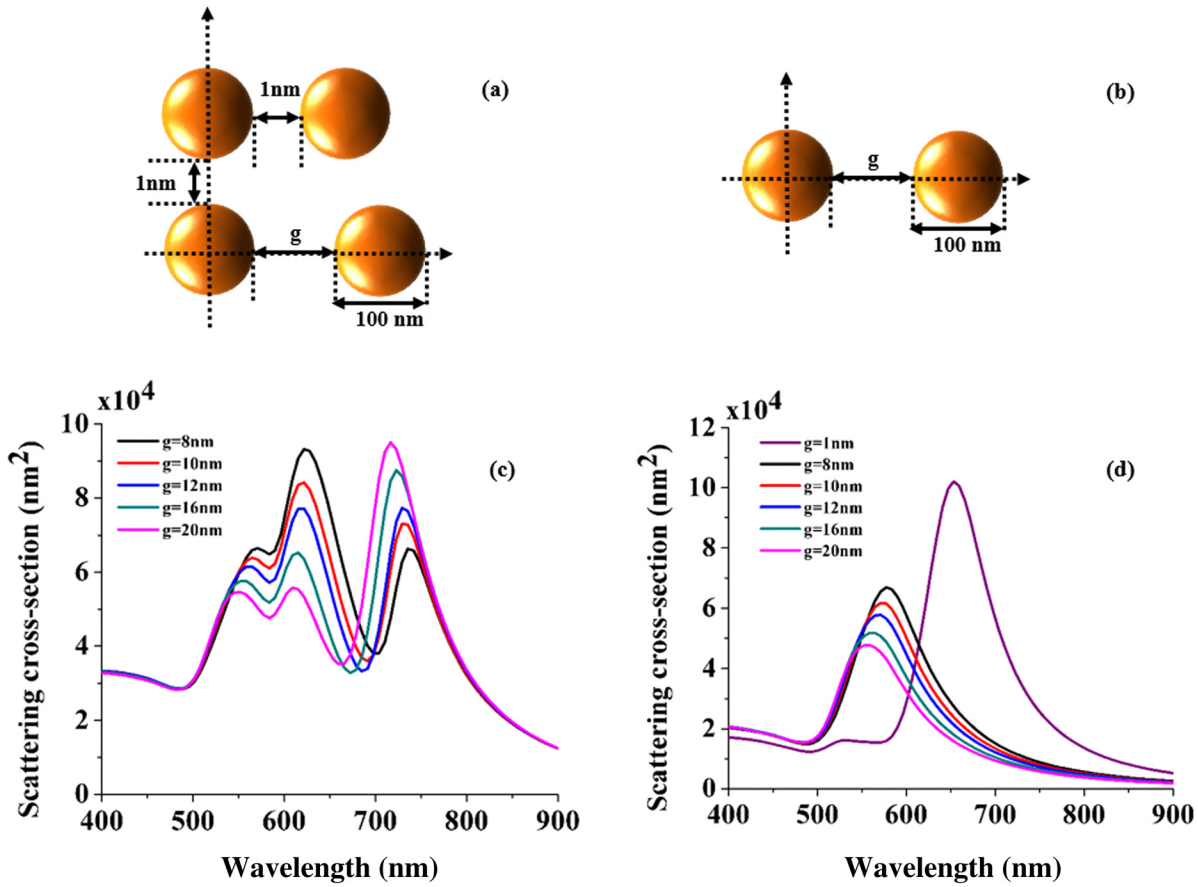

FIG. 6. Scattering cross-section of asymmetric Au metamolecules and individual constituent dimer components for various inter-particle gaps g under s-polarization. Dual Fano dips generated by the interference of bright and dark modes of individual dimers in asymmetric metamolecules.

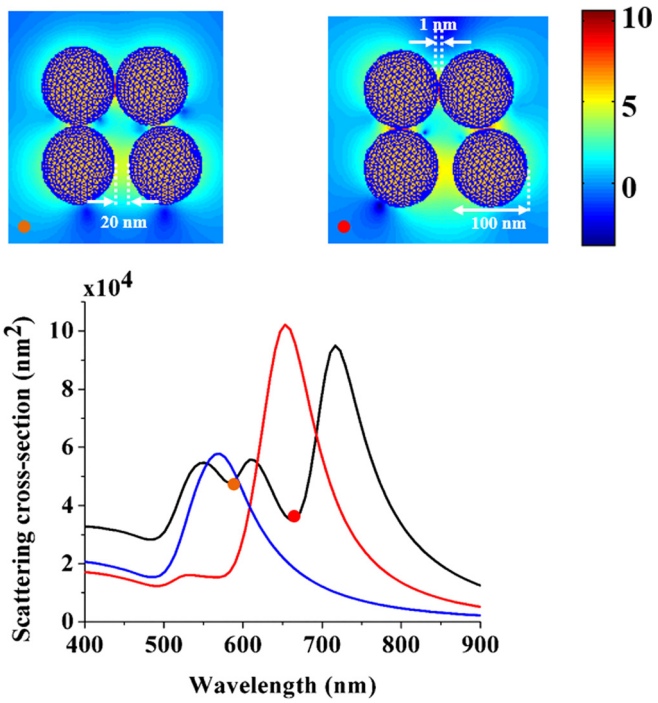

FIG. 7. Scattering cross-section of individual dimers and asymmetric Au metamolecules under s-polarization. Logarithm scale of relative electric field intensity (log ($|E|^2/|E_0|^2$) at Fano dips demonstrates the plasmonic coupling of dimers.

full width at half maximum (FWHM) centered at the considered resonant wavelength (FOM = S/FWHM).[10] Table I shows the optical properties of the proposed optical sensor. The resonant wavelength at the SCS's peaks and dip increases when the refractive index of the surrounding environment increases. There is a trade-off between sensitivity and selectivity in choosing the optimal sensor. In sensing applications, a sensor with high FOM is desirable. Therefore, based on the Fano dip, a sensor having FOM of 4.7 appears ideal.

Recently, we have demonstrated that with a metasurface induced Fano resonance it may be possible to enhance solar absorption in thin-film organic solar cells at the 600–800 nm wavelength range, where the polymer absorption efficiency is itself small in the absence of external effects.[61] A metasurface consisting of asymmetric-arranged nanopillars was therefore proposed to be integrated into the active layer. The induced Fano resonance plays a dominant role when combined with LSPRs around nanopillars to boost absorption efficiency. In this operation, a strong field enhancement in the gap between neighboring nanoparticle is responsible for the absorption enhancement. Since the Fano resonance is responsible for this effect, the ability to generate multiple Fano resonances in the proposed metamolecules undoubtedly makes them ideal candidates to enhance thin-film solar cell absorption. In addition, the metamolecule may inspire the

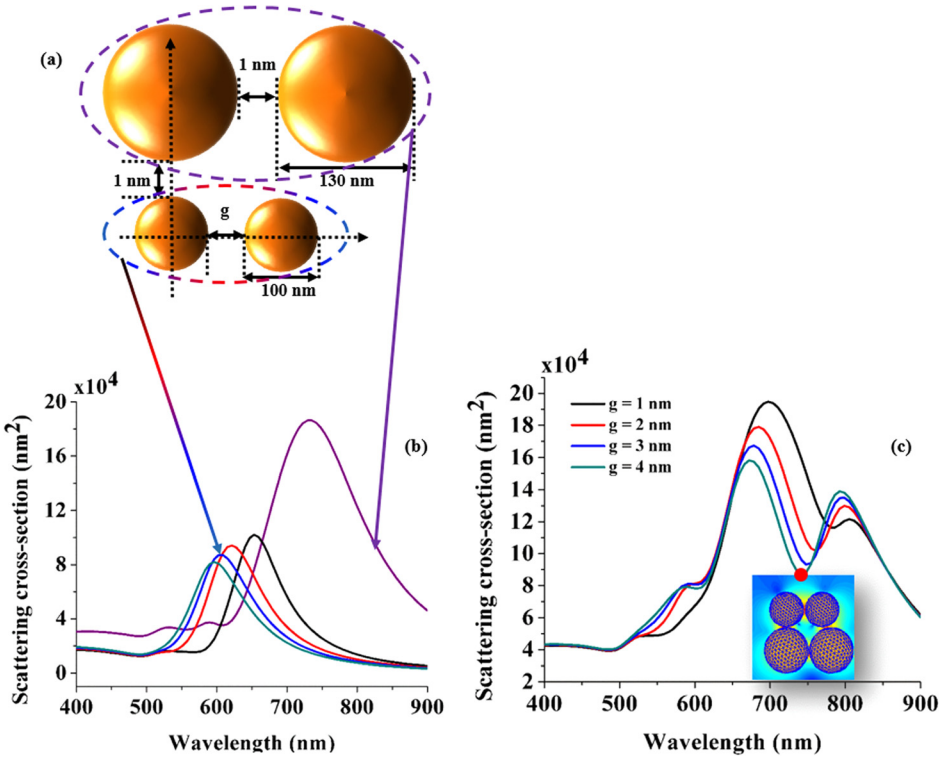

FIG. 8. Scattering cross-section of asymmetric Au metamolecules and individual dimer components for various inter-particle gaps g under s-polarization. Dual Fano dips generated by the interference of bright and dark modes of individual dimers in asymmetric metamolecules. Logarithm scale of relative electric field intensity ($\log(|E|^2/|E_0|^2)$) at the indicated Fano dip demonstrates the plasmonic coupling of dimers.

design of metamaterial-based absorbers for thermophotovoltaic applications.[62] In the past, a great deal of research has been presented to realize these absorbers based on the coupling of a single metallic nanoparticle to a metallic thin-film.[63] At a single nanoparticle's LSPR, a strong field confinement in the area between the nanoparticle and film results in an exceptional near-unity absorption. However, the large absorption was limited to a narrow bandwidth. This may be potentially overcome by coupling the proposed metamolecule with metallic thin-films, since the induced multiple Fano resonances will provide several absorbing peaks leading to the realization of broadband metamaterial-based solar absorbers.

The other potential application of the proposed metamolecule may reside in enhanced photon up-conversion (UC). Failure to absorb photons below the bandgap of active materials (i.e., GaAs or Si) in single-junction solar cells limits the power conversion efficiency below the Shockley-Queisser limit at about 32%.[64] UC of these low-energy photons provides the possibility to surpass this thermodynamic efficiency limit. However, UC materials have very limited impact in photovoltaic cells due to their extremely weak and narrow near-IR absorption band.[65] Therefore, it is necessary to explore solar cell architectures delivering ultrahigh light intensities in the IR to the UC material and to broaden the UC spectrum. With the ability to generate and shift multiple Fano resonances into the IR in addition to the associated strong electric field enhancement at these resonances, it is suggested that it may be possible to significantly enhance UC efficiency by properly positioning the metamolecules into the UC materials, and thus improve the power conversion efficiency of photovoltaic devices.

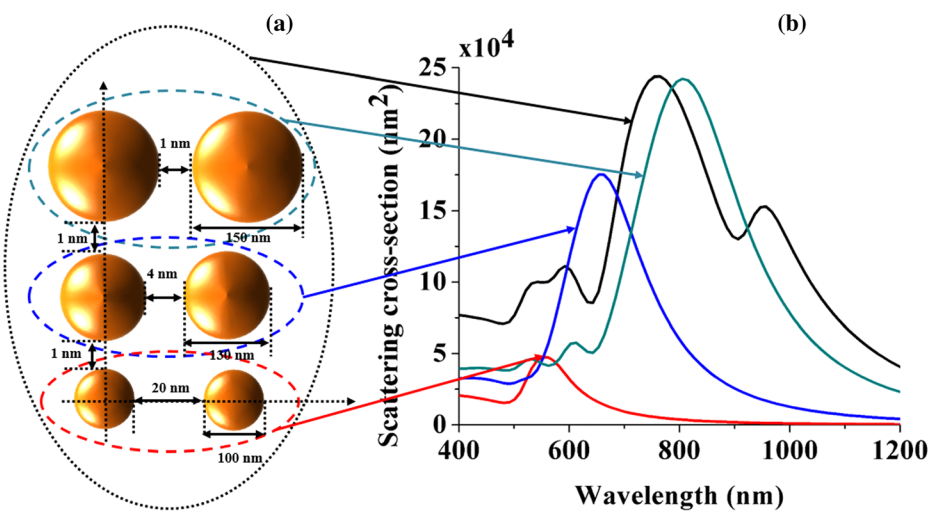

FIG. 9. Scattering cross-section of asymmetric Au metamolecule and individual dimer components under s-polarization. Multiple Fano dips generated by the interference of bright and dark modes of individual dimers in the metamolecule.

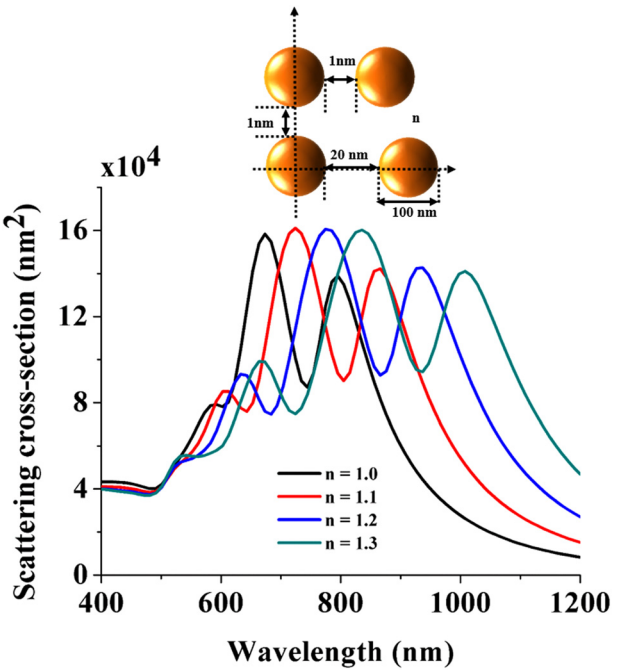

FIG. 10. Refractive index sensitivity of scattering cross-section of asymmetric Au metamolecules under s-polarization.

TABLE I. Optical properties of metamolecule-based refractive index sensor.

Refractive index, n		1.0	1.1	1.2	1.3
Peak 1	Resonant wavelength (nm)	675	725	779	834
	Q-factor	5.7	4.7	4.4	4.1
	Sensitivity (nm/RIU)		S = 530		
	FOM		FOM = 3.3		
Peak 2	Resonant wavelength (nm)	794	865	935	1008
	Q-factor	6.0	5.9	5.6	5.5
	Sensitivity (nm/RIU)		S = 713		
	FOM		FOM = 4.5		
Dip	Fano dip (nm)	744	805	865	936
	Q-factor	7.5	6.1	5.7	5.2
	Sensitivity (nm/RIU)		S = 640		
	FOM		FOM = 4.7		

IV. CONCLUSION

In this paper, we have demonstrated the interference of bright and dark modes of constituent dimers of the metamolecule to generate and control single and multiple Fano resonances. The sharpness of the resulting Fano dip depends on the contrast of these interacting modes. Proper positioning of the constituent dimers in the metamolecules results in multiple Fano resonances that can be tuned by varying the size and gap of the dimers, providing flexibility for their potential applications in refractive index sensing, energy-harvesting, and photon up-conversion.

ACKNOWLEDGMENTS

The authors would like to appreciate Dr. Quang Minh Ngo, Vietnam Academy of Science and Technology, for his valuable comments and suggestions in this work.

[1]N. A. Mirin, K. Bao, and P. Nordlander, J. Phys. Chem. A **113**, 4028–4034 (2009).
[2]J. B. Lassiter, H. Sobhani, J. A. Fan, J. Kundu, F. Capasso, P. Nordlander, and N. J. Halas, Nano Lett. **10**, 3184–3189 (2010).
[3]J. A. Fan, K. Bao, C. Wu, J. Bao, R. Bardhan, N. J. Halas, V. N. Manoharan, G. Shvets, P. Nordlander, and F. Capasso, Nano Lett. **10**, 4680–4685 (2010).
[4]B. Luk'yanchuk, N. I. Zheludev, S. A. Maier, N. J. Halas, P. Nordlander, H. Giessen, and C. T. Chong, Nature Mater. **9**, 707–715 (2010).
[5]A. E. Miroshnichenko, S. Flach, and Y. S. Kivshar, Rev. Mod. Phys. **82**, 2257–2298 (2010).
[6]C. Wu, A. B. Khanikaev, and G. Shvets, Phys. Rev. Lett. **106**, 107403 (2011).
[7]M. Rahmani, B. Luk'yanchuk, and M. Hong, Laser Photonics Rev. **7**, 1–21 (2012).
[8]W. S. Chang, J. B. Lassiter, P. Swanglap, H. Sobhani, S. Khatua, P. Nordlander, N. J. Halas, and S. Link, Nano Lett. **12**, 4977–4982 (2012).
[9]C. Wu, A. B. Khanikaev, R. Adato, N. Arju, A. A. Yanik, H. Altug, and G. Shvets, Nature Mater. **11**, 69 (2012).
[10]J. Wang, C. Fan, J. He, P. Ding, E. Liang, and Q. Xue, Opt. Express **21**, 2236–2244 (2013).
[11]Y. Zhan, D. Y. Lei, X. Li, and S. A. Maier, Nanoscale **6**, 4705 (2014).
[12]J. A. Fan, C. Wu, K. Bao, J. Bao, R. Bardhan, N. J. Halas, V. N. Manoharan, P. Nordlander, G. Shvets, and F. Capasso, Science **328**, 1135 (2010).
[13]M. Hentchel, M. Saliba, R. Vogelgesang, H. Giessen, A. P. Alivisatos, and N. Liu, Nano Lett. **10**, 2721 (2010).
[14]S. Zhang, D. A. Genov, Y. Wang, M. Liu, and X. Zhang, Phys. Rev. Lett. **101**, 047401 (2008).
[15]N. Verellen, Y. Sonnefraud, H. Sobhani, F. Hao, V. V. Moshchalkov, P. Van Dorpe, P. Nordlander, and S. A. Maier, Nano Lett. **9**, 1663 (2009).
[16]Y. Hu, S. J. Noelck, and R. A. Drezek, ACS Nano **4**, 1521–1528 (2010).
[17]A. Artar, A. A. Yanik, and H. Altug, Nano Lett. **11**, 3694–3700 (2011).
[18]G. Bachelier, I. Russier-Antoine, E. Benichou, C. Jonin, N. Del Fatti, F. Vallee, and P.-F. Brevet, Phys. Rev. Lett. **101**, 197401 (2008).
[19]Z.-J. Yang, Z.-S. Zhang, W. Zhang, Z.-H. Hao, and Q.-Q. Wang, Appl. Phys. Lett. **96**, 131113 (2010).
[20]Z.-J. Yang, Z.-S. Zhang, W. Zhang, Z.-H. Hao, and Q.-Q. Wang, Appl. Phys. Lett. **99**, 081107 (2011).
[21]F. Hao, Y. Sonnefraud, P. Van Dorpe, S. A. Maier, N. J. Halas, and P. Nordlander, Nano Lett. **8**, 3983 (2008).
[22]F. Hao, P. Nordlander, Y. Sonnefraud, P. Van Dorpe, and S. A. Maier, ACS Nano **3**, 643 (2009).
[23]Y. Sonnefraud, N. Verellen, H. Sobhani, G. A. E. Vandenbosch, V. V. Moshchalkov, P. Van Dorpe, P. Nordlander, and S. A. Maier, ACS Nano **4**, 1664 (2010).
[24]S. Mukherjee, H. Sobhani, J. B. Lassiter, R. Bardhan, P. Nordlander, and N. J. Halas, Nano Lett. **10**, 2694–2701 (2010).
[25]D. Wu, S. Jiang, and X. Liu, J. Chem. Phys. **136**, 034502 (2012).
[26]C. Argyropoulos, F. Monticone, G. D'Aguanno, and A. Alù, Appl. Phys. Lett. **103**, 143113 (2013).
[27]Z. Y. Fang, J. Cai, Z. yan, P. Nordlander, N. J. Halas, and X. Zhu, Nano Lett. **11**, 4475–4479 (2011).
[28]F. Shafiei, F. Monticone, K. Q. Le, X.-X. Liu, T. Hartsfield, A. Alù, and X. Li, Nat. Nanotechnol. **8**, 95–99 (2013).
[29]V. A. Fedotov, M. Rose, S. L. Provirnin, N. Papasimakis, and N. I. Zheludev, Phys. Rev. Lett. **99**, 147401 (2007).
[30]D. Dregely, M. Hentschel, and H. Giessen, ACS Nano **5**, 8202–8211 (2011).
[31]S.-D. Liu, Z. Yang, R.-P. Liu, and X.-Y. Li, ACS Nano **6**, 6260–6271 (2012).
[32]J. Chen, Q. Shen, Z. Chen, Q. Wang, C. Wang, C. Tang, and Z. Wang, J. Chem. Phys. **136**, 214703 (2012).
[33]A. F. Oskooi, D. Roundy, M. Ibanescu, P. Bermel, J. D. Joannopoulos, and S. G. Johnson, Comput. Phys. Commun. **181**, 687–702 (2010).
[34]J. Jin, *The Finite Element Method in Electromagnetics*, 2nd ed. (Wiley, New York, 2002).
[35]F. J. Garcia de Abajo and A. Howie, Phys. Rev. B **65**, 115418 (2002).
[36]F. J. Garcia de Abajo, Rev. Mod. Phys. **82**, 209 (2010).
[37]M. El-Shenawee, IEEE Trans. Antennas Propag. **51**, 802–809 (2003).
[38]U. Hohenester and A. Trugler, Comput. Phys. Commun. **183**, 370–381 (2012).
[39]P. B. Johnson and R. W. Christy, Phys. Rev. B **6**, 4370 (1972).

[40]R. Esteban, A. G. Borisov, P. Nordlander, and J. Aizpurua, Nat. Commun. **3**, 825 (2012).
[41]K. J. Savage, M. M. Hawkeye, E. Esteban, A. G. Borisov, J. Aizpurua, and J. J. Baumberg, Nature **491**, 574–577 (2012).
[42]T. V. Teperik, P. Nordlander, J. Aizpurua, and A. G. Borisov, Opt. Express **21**, 27306–27325 (2013).
[43]H. Cha, J. H. Yoon, and S. Yoon, ACS Nano **8**, 8554–8563 (2014).
[44]I. Romero, J. Aizpurua, G. W. Bryant, and F. J. Garcia de Abajo, Opt. Express **14**, 9988–9999 (2006).
[45]W. Rechberger, A. Hohenau, A. Leitner, J. R. Krenn, B. Lamprecht, and F. R. Aussenegg, Opt. Commun. **220**, 137–141 (2003).
[46]E. Hao and G. C. Schatz, J. Chem. Phys. **120**, 357–366 (2004).
[47]A. Alù and N. Engheta, Phys. Rev. B **78**, 195111–195116 (2008).
[48]M. El-Shenawee, IEEE Antennas Wireless Propag. Lett. **9**, 463–466 (2010).
[49]C.-Y. Tsai, J.-W. Lin, C.-Y. Wu, P.-T. Lin, T.-W. Lu, and P. T. Lee, Nano Lett. **12**, 1648–1654 (2012).
[50]A. Polemi and K. L. Shuford, J. Chem. Phys. **136**, 184703 (2012).
[51]L. Silbertsein, Philos. Mag. **33**, 92–128 (1917); **33**, 215–222 (1917); **33**, 521–533 (1917).
[52]B. T. Thole, Chem. Phys. **59**, 341–350 (1981).
[53]O. N. Gadomskii and Y. Y. Voronov, J. Appl. Spectrosc. **66**, 882–889 (1999).
[54]O. N. Gadomsky, S. V. Sukhov, and Y. Y. Voronov, Eur. Phys. J. D **11**, 185–190 (2000).
[55]M. V. Rybin *et al.*, Phys. Rev. B **88**, 205106 (2013).
[56]K. Q. Le and P. Bienstman, IEEE Photon. J. **3**, 538–545 (2011).
[57]B. Gallinet and O. J. F. Martin, ACS Nano **7**, 6978–6987 (2013).
[58]K. Q. Le, J. Appl. Phys. **114**, 084504 (2013).
[59]K. Q. Le and S. John, Opt. Express **22**, A1–A12 (2014).
[60]A. B. Khanikaev, C. Wu, and G. Shvets, Nanophotonics **2**, 247–264 (2013).
[61]K. Q. Le and A. Alù, Appl. Phys. Lett. **105**, 141118 (2014).
[62]C. Wu, B. Neuner III, J. John, A. Milder, B. Zollers, S. Savoy, and G. Shvets, J. Opt. **14**, 024005 (2012).
[63]C. M. Watts, X. Liu, and W. J. Padilla, Adv. Mater. **24**, OP98–OP120 (2012).
[64]G. Güttler and H. J. Quessier, Energy Convers. **10**, 51–55 (1970).
[65]W. Zou, C. Visser, J. A. Maduro, M. S. Pshenichnikov, and J. C. Hummelen, Nat. Photonics **6**, 560–564 (2012).